

# On the $TE_{n0}$ Modes of a Ferrite Slab Loaded Rectangular Waveguide and the Associated Thermodynamic Paradox\*

A. D. BRESLER†

**Summary**—It has been known for some time that the secular equation for the  $TE_{n0}$  modes of a perfectly conducting rectangular waveguide loaded with a transversely magnetized dissipationless full height ferrite slab located against one of the narrow walls of the waveguide admits the possibility of the existence of only a single propagating mode (transporting energy in one direction only). In this paper, it is established that if we admit the existence of a passive dissipationless uniform waveguide supporting only a single propagating mode we are led inescapably to a thermodynamic paradox. A uniqueness theorem is cited to establish that, for the waveguide described above, the paradox is associated with the  $TE_{n0}$  mode set alone. This conclusion motivates a thorough study of the secular equation for the  $TE_{n0}$  modes of this waveguide. This study is initiated by an investigation into the properties of the  $TE_{n0}$  surface waves guided along a plane interface separating a transversely magnetized dissipationless ferrite from free space. It is shown that two oppositely directed surface waves are guided along this interface. These two surface waves are admitted in different finite ranges of the parameter values which never coincide and which may or may not overlap. Each of the two surface waves has both a high- and a low-frequency cutoff and, in general, both a high and a low dc magnetic field cutoff. The propagation constant of one of the surface waves becomes infinite at the low field (high-frequency) cutoff. The next step in the analysis consists of an examination of the behavior of these surface waves on finite thickness ferrite slabs located in different environments. It is shown that when one of the two interfaces bounding the slab approaches a short circuit the infinite propagation constant noted above behaves in a peculiar discontinuous fashion. Next, the  $TE_{n0}$  mode secular equation of the slab loaded rectangular waveguide is analyzed and information is developed leading to a description of the behavior of the propagation constants of all the propagating  $TE_{n0}$  modes. This analysis reveals that the possibility of the existence of only a single propagating mode is associated only with the surface wave mode of this waveguide. A resolution for the thermodynamic paradox is proposed based on the discontinuous behavior of one of the infinite propagation constants associated with this surface wave mode. It is shown that with a properly chosen secular equation for the waveguide under consideration there are always an even number of  $TE_{n0}$  propagating modes, half of which transport energy in one direction, half in the other. This demonstration is based, in part, on an analysis leading to relations between the direction of the power flow associated with a propagating mode and the derivative of its propagation constant with respect to the dc magnetic field.

\* Manuscript received by the PGMTT, April 6, 1959; revised manuscript received, September 2, 1959. Parts of this paper were presented at the IRE-URSI meeting, Washington, D. C., April, 1958. It is based, in part, on the author's dissertation submitted to the Polytechnic Institute of Brooklyn, Brooklyn, N. Y., in partial fulfillment of the requirements for the degree of Doctor of Engineering. The work on which this paper is based was done while the author was a member of the staff of the Microwave Res. Inst. of the Polytechnic Institute of Brooklyn, and was supported by the Air Force Cambridge Res. Center under contract AF-19(604)-2301.

† Jasik Laboratories, Inc., 100 Shames Dr., Westbury, N. Y.

## INTRODUCTION—THE THERMODYNAMIC PARADOX

THIS PAPER is concerned with a study of the  $TE_{n0}$  modes<sup>1</sup> of a perfectly conducting rectangular waveguide loaded with a full height ferrite slab located against one of the narrow walls of the waveguide. The ferrite slab is uniformly magnetized in the transverse direction indicated in Fig. 1. As part of this study, we will examine the properties of the  $TE_{n0}$  surface wave modes guided along the plane interfaces separating transversely magnetized ferrite slabs from free space. While these studies are of interest in their own right, they also have a further significance which will now be made evident by a statement of their motivation.

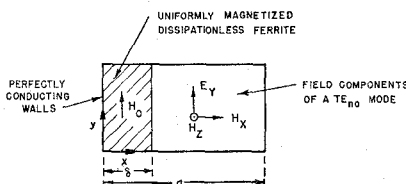


Fig. 1—Ferrite slab loaded rectangular waveguide (slab against waveguide wall).

Some time ago, Lax and Button<sup>2</sup> pointed out a curious phenomenon associated with the spectrum of the waveguide whose cross section is shown in Fig. 1. They found that the secular equation determining the propagation constants of the  $TE_{n0}$  modes of this waveguide admitted the possibility of the existence of only a single propagating mode (transporting energy in one direction only). The obvious implication is that this waveguide can be used to construct an ideal one way transmission system. If this were really possible, it would constitute a clear violation of the basic laws of thermodynamics. In

<sup>1</sup> These modes are characterized by the absence of any variation along the direction of the dc magnetic field,  $H_0$ , and by the fact that the electric field is parallel to  $H_0$ . The locations of the conducting planes normal to the  $y$  direction are therefore of no significance. For a description of the field components see, e.g., H. Seidel, "Ferrite slabs in transverse electric mode waveguide," *J. Appl. Phys.*, vol. 28, pp. 218-226; February, 1957.

<sup>2</sup> B. Lax and K. J. Button, "Theory of new ferrite modes in rectangular waveguide," *J. Appl. Phys.*, vol. 26, pp. 1184-1185; September, 1955. Also, "Theory of ferrites in rectangular waveguide," *IRE TRANS. ON ANTENNAS AND PROPAGATION*, vol. AP-4, pp. 531-537; July, 1956.

an attempt to resolve this difficulty, it has been argued<sup>3,4</sup> that the power flow in the reverse direction takes place via the cutoff (nonpropagating) modes and that therefore no thermodynamic difficulty actually exists. We will now show that the cutoff modes do not provide a satisfactory mechanism for the resolution of the paradox. This demonstration will not be restricted to the special case of the waveguide described previously.

To establish that the existence of a passive dissipationless uniform waveguide supporting only a single propagating mode does indeed constitute a violation of the basic thermodynamic laws, we note the following. First, we recall that in a dissipationless waveguide only the propagating modes (considered individually) carry power.<sup>5</sup> The cutoff modes take part in the mechanism of energy transport only through the coupling between two modes associated with complex conjugate propagation constants.<sup>5</sup> Now, consider the junction of the two dissimilar uniform waveguides illustrated in Fig. 2. In an earlier paper,<sup>6</sup> the author has shown that when this structure is excited from the empty waveguide side the fields to the right of the junction plane will consist of a superposition of only those modes which, if propagating, transport energy to the right (*i.e.*, along  $+z$ ) or, if cut off, decay exponentially with increasing  $z$ . Thus, only one of the two modes associated with a pair of complex conjugate propagation constants is excited at the junction plane and therefore the cutoff modes play no role in the transport of energy away from the junction. Finally, suppose that the waveguide to the right of the junction plane supports only a single propagating mode which (without loss of generality) is assumed to transport energy to the right. The incident wave shown in Fig. 2 would then excite this single propagating mode along with an infinity of cutoff modes which all decay with increasing  $z$ . Therefore, for  $z \gg z'$  and increasing, the fields in the waveguide approach ever more closely to the propagating mode fields.

Now let a short circuit termination be introduced into the waveguide at some  $z \gg z'$ . Since there are no prop-

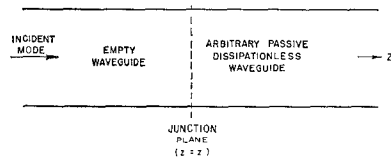


Fig. 2—Junction of two dissimilar uniform waveguides.

<sup>3</sup> B. Lax, Chairman, "Combined panel session on propagation in doubly-refracting media and future directions for research in electromagnetic wave theory in modern physics," IRE TRANS. ON ANTENNAS AND PROPAGATION, vol. 4, pp. 567-577 (esp. 573-576); July, 1956.

<sup>4</sup> M. L. Kales, "Topics in guided wave propagation in magnetized ferrites," PROC. IRE, vol. 44, pp. 1403-1409; October, 1956. The discussion referred to appears on p. 1408.

<sup>5</sup> A. D. Bresler, G. H. Joshi, and N. Marcuvitz, "Orthogonality properties for modes in passive and active uniform waveguides," *J. Appl. Phys.*, vol. 29, pp. 794-799; May, 1958.

<sup>6</sup> A. D. Bresler, "The far fields excited by a point source in a passive dissipationless anisotropic waveguide," IRE TRANS. ON MICROWAVE THEORY AND TECHNIQUES, vol. 7, pp. 282-287; April, 1959.

agating modes which carry power to the left, only cutoff modes will be excited at the short circuit. The amplitude coefficients of these cutoff modes will be determined from the requirement that the net tangential electric field at the short circuit must equal zero. Admittedly, some power transfer now takes place via the coupling between pairs of cutoff modes which decay with equal attenuations in opposite directions along  $z$ .<sup>5</sup> To demonstrate that this power transfer mechanism cannot provide a proper power balance, we first assume the converse; *i.e.*, we assume that the net power flow through the transverse plane just to the left of the short circuit is equal to zero. This net power flow may be written as  $P_0 + \Sigma P_i$ , where  $P_0$  is the power flow associated with the single propagating mode and  $\Sigma P_i$  is the net power flow resulting from cutoff mode coupling. Each term in  $\Sigma P_i$  is proportional to the product of the amplitude coefficients of a pair of cutoff modes characterized by complex conjugate propagation constants one of which is excited at the junction plane, the other at the short circuit.<sup>5,6</sup> Now suppose that the short circuit is moved a distance  $n\lambda_{g0}$  ( $n$  is an integer,  $\lambda_{g0}$  is the guide wavelength associated with the propagating mode) further away from  $z'$ . The fields incident on the short circuit in the two locations are almost identical. Thus, for either location, the set of modes excited at the short circuit constitutes a modal representation (in terms of a complete eigenfunction set) of a transverse electromagnetic field whose electric field component must be almost exactly the negative of the propagating mode transverse electric field incident on the short circuit. Since the two short circuit positions are separated by  $n\lambda_{g0}$ , this latter field has equal amplitudes at the two short circuit positions. Therefore, the amplitude coefficients of the cutoff modes excited at the short circuit are practically identical for the two locations. In traversing the distance between the two short-circuit positions, the cutoff modes excited at  $z'$  are attenuated by the factor  $\exp(-\alpha_i n \lambda_{g0})$  where  $\alpha_i > 0$  is the attenuation constant of the  $i$ th mode. Thus, if we now compute the net power flow through the transverse plane just to the left of the new short-circuit position, we find that  $P_0$  is unchanged while each term in  $\Sigma P_i$  is reduced by the factor  $\exp(-\alpha_i n \lambda_{g0})$ . Therefore  $P_0 + \Sigma P_i$  is now unequal to zero. We must therefore conclude that power transfer via cutoff mode coupling cannot provide the proper power balance. Thus, when we introduce the short circuit termination we are faced with a situation wherein we are continuously pumping energy into a reactive termination and no means exists for returning all of this energy to the source. This clearly constitutes a violation of the basic laws of thermodynamics. We are therefore led to assert that a passive dissipationless uniform waveguide cannot support but a single propagating mode.

We are now faced with the problem of reconciling this assertion with the known results cited earlier for the waveguide in Fig. 1. In this connection, it is important to recognize that when the discontinuity problem posed

in Fig. 2 is that for an infinite rectangular waveguide which is empty for  $z < z'$  and which, for  $z > z'$ , is loaded with a ferrite slab as in Fig. 1, then the paradox arises even though it is the  $TE_{n0}$  mode set of the slab loaded waveguide which has only a single propagating mode. This conclusion is based on a uniqueness theorem established by the author<sup>7</sup> which states that if the fields which excite the two waveguides are independent of  $y$  (see Fig. 1) and are completely characterized by a single non-zero component of electric field directed along  $y$ , then the boundary value problem which has been posed is actually a two dimensional problem and the total field in the structure can be completely described in terms of this single component of electric field. Thus, when the incident mode indicated in Fig. 2 is, e.g., the  $TE_{10}$  mode of the empty rectangular waveguide, only  $TE_{n0}$  modes will be excited at the junction plane and we therefore may not look outside the  $TE_{n0}$  mode set to resolve our difficulty.

In casting about for a basis for resolving this paradox, we reject the approach advanced by Seidel<sup>8,9</sup> which involves the assumption of an "intrinsic loss" for a lossless ferrite medium and into which he introduces arguments based on a consideration of the atomic model from which the ferrite properties are deduced. Our attitude is that such arguments seek to answer an electromagnetic question by considerations outside the framework in which the problem is posed. To be more specific, our attitude is that we are concerned solely with the solutions to the Maxwell equations in a region containing an anisotropic medium for which we are given the permeability dyadic. We do not need to know the atomic model from which this dyadic has been deduced. We do know that this dyadic satisfies the restrictions imposed by the linearity, passivity, losslessness and time reversibility requirements.<sup>6,10</sup> Under these circumstances, if the solutions to the Maxwell equations give rise to thermodynamic difficulties, the source of the difficulties must be sought in the electromagnetic problem, not in the atomic model.

As a consequence of the considerations outlined above a thorough analysis of the  $TE_{n0}$  modes of the waveguide illustrated in Fig. 1 was undertaken. As a result of this analysis, we will establish that with a properly chosen secular equation for the waveguide in Fig. 1 there are always an even number of  $TE_{n0}$  propagating modes, half of which transport energy in one direction, half in the other. This will dispose of the thermodynamic paradox associated with this structure. To accomplish this task,

<sup>7</sup> A. D. Bresler, "On the Discontinuity Problem at the Input to an Anisotropic Waveguide," D.E.E. dissertation, Polytechnic Institute of Brooklyn, Brooklyn, N. Y.; June, 1959. The dissertation has also appeared as Res. Rept. No. R-716-59 of the Microwave Res. Inst. of the Polytechnic Inst. of Brooklyn.

<sup>8</sup> Seidel, *op. cit.*

<sup>9</sup> "Round-table discussion on design limitations of microwave ferrite devices," IRE TRANS. ON MICROWAVE THEORY AND TECHNIQUES, vol. 6, pp. 104-111; January, 1958.

<sup>10</sup> B. S. Gourary, "Dispersion relations for tensor media and their application to ferrites," *J. Appl. Phys.*, vol. 28, pp. 283-288; March, 1957.

we will first show that the possibility of the existence of only a single propagating mode is associated only with the surface wave mode, *i.e.*, the "ferrite-dielectric" mode identified by Lax and Button.<sup>2</sup> In the discussion which follows, we will first examine the properties of this surface-wave mode. This mode represents a true surface phenomenon in that the amplitudes of its fields decay exponentially away from the ferrite-empty space interface on both sides of the interface. Therefore, the essential properties of this surface wave mode will be determined from a study of its behavior in the ferrite loaded parallel plate waveguide, whose cross section is shown in Fig. 3.

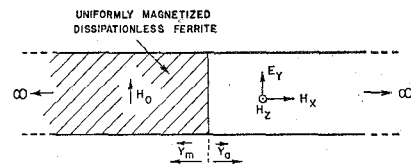


Fig. 3—Ferrite loaded parallel plate waveguide.

#### DEFINITIONS AND PRELIMINARY CONSIDERATIONS

All field components are assumed to have the (suppressed) time dependence  $\exp(-i\omega t)$  where  $\omega$  is the radian frequency. Since we will be concerned exclusively with  $TE_{n0}$  modes, all field components are independent of  $y$ . Since these modes propagate along  $z$ , the  $z$  dependence for all field components in either the empty or ferrite loaded regions is taken as  $\exp(ikz)$ . The dependence on  $x$  differs in the two regions. This dependence is taken as  $\exp(\pm ik_{xa}x)$  in the empty regions and  $\exp(\pm ik_{xm}x)$  in the ferrite loaded regions. We adopt the convention that both  $k_{xa}$  and  $k_{xm}$  satisfy the restrictions  $k_x > 0$  if real and  $\text{Im } k_x > 0$  if imaginary. The wave numbers  $\kappa$  and  $k_x$  are related via<sup>1</sup>

$$\kappa^2 = k^2 - k_{xa}^2 = k^2 \epsilon \nu_1 - k_{xm}^2 \quad (1)$$

where  $k^2 = \omega^2 \mu_0 \epsilon_0$ ,  $\mu_0$  and  $\epsilon_0$  are, respectively, the permeability and permittivity of free space,  $\epsilon$  is the (relative) scalar dielectric constant of the ferrite and  $\nu_1$ , the (relative) effective permeability parameter for transverse magnetization, will be defined more precisely below.

For the time dependence indicated above, the (relative) permeability tensor for a gyromagnetic ferrite subjected to a uniform internal magnetic field applied along  $y$  takes the form<sup>11</sup>

$$\mathbf{u}_{zxy} = \begin{bmatrix} \mu_1 & i\mu_2 & 0 \\ -i\mu_2 & \mu_1 & 0 \\ 0 & 0 & 1 \end{bmatrix} \quad (2)$$

where the subscripts on  $\mathbf{u}$  indicate the cyclic order employed in the tensor representation. For a dissipationless ferrite, the dependence of  $\mu_{1,2}$  on frequency, dc magnetic field ( $H_0$ ), and saturation magnetization of the ferrite ( $4\pi M_s$ ) is given by<sup>11</sup>

<sup>11</sup> H. Suhl and L. R. Walker, "Topics in guided wave propagation through gyromagnetic media," *Bell Sys. Tech. J.*, vol. 33, pp. 579-660; May, 1954.

$$\mu_1 = \frac{1 - \sigma(\rho + \sigma)}{1 - \sigma^2} \quad \mu_2 = \frac{\rho}{1 - \sigma^2} \quad (3)$$

where

$$\rho = \frac{\gamma(4\pi M_s)}{\omega} \quad \sigma = \frac{\gamma H_0}{\omega} \quad (4)$$

and  $\gamma$  is the magnitude of the gyromagnetic ratio.<sup>12</sup> Note that  $\rho$  and  $\sigma$  are defined so that at a fixed frequency  $\rho$  is a constant of the material while  $\sigma$  is proportional to the dc magnetic field. Eqs. (3) are valid only for saturated ferrites, *i.e.*, only when  $H_0$  exceeds that value required to produce saturation. Since the dc permeability of most ferrites is very large, the value of  $\sigma$  required for saturation is very small.<sup>11</sup> Thus, whenever results are stated for  $\sigma=0$  these are understood to be valid when  $\sigma$  approaches zero but remains larger than the value required for saturation. Since  $H_0$  and  $4\pi M_s$  must have the same algebraic sign, it follows that the product  $\rho\sigma$  is always positive. Therefore, a reversal of the dc magnetic field changes the sign of  $\mu_2$  but does not affect  $\mu_1$ .

For modes which propagate in a direction perpendicular to the dc magnetic field, it is convenient to express all results in terms of the elements of the inverse  $\mathbf{y}$  tensor

$$\mathbf{y}^{-1} = \begin{pmatrix} 1 & -i & 1 \\ \frac{1}{\nu_1} & \frac{1}{\nu_2} & 0 \\ i \frac{1}{\nu_2} & \frac{1}{\nu_1} & 0 \\ 0 & 0 & 1 \end{pmatrix} \quad (5)$$

where

$$\begin{aligned} \nu_1 &= \frac{\mu_1^2 - \mu_2^2}{\mu_1} = \frac{1 - (\rho + \sigma)^2}{1 - \sigma(\rho + \sigma)} \\ \nu_2 &= \frac{\mu_1^2 - \mu_2^2}{\mu_2} = \frac{1 - (\rho + \sigma)^2}{\rho} \end{aligned} \quad (6)$$

It is evident that a reversal of the dc magnetic field changes the sign of  $\nu_2$  but does not affect  $\nu_1$ . The parameters  $\mu_{1,2}$  and  $\nu_{1,2}$  are sketched in Fig. 4 as functions of  $\sigma$  for fixed  $\rho$ . These sketches therefore illustrate the behavior of the permeability as a function of the dc magnetic field for a fixed ferrite at a fixed frequency.

Certain features of the curves in Fig. 4 deserve comment. First, since (3) and (6) are valid only for saturated ferrites, we should not be disturbed by the fact that the curves based on these equations do not indicate an isotropic medium at  $\sigma=0$ . On the other hand, Fig. 4 makes evident that the ferrite becomes an isotropic dielectric as  $\sigma$  approaches infinity. Next, we remark that at  $\sigma=1$ , *i.e.*, at the ordinary "gyromagnetic resonance," the parameters  $\nu_{1,2}$  do not display any resonance or, indeed, any sort of unusual behavior. We will find that the point  $\sigma=1$  has no significance for the surface wave phenomena. Finally, two special values of  $\sigma$ ,  $\sigma_2$ , and  $\sigma_5$  are indi-

<sup>12</sup>  $\gamma=5.6\pi$  for  $H_0$  expressed in kilo-oersted,  $4\pi M_s$  in kilogauss and frequency in kmc.

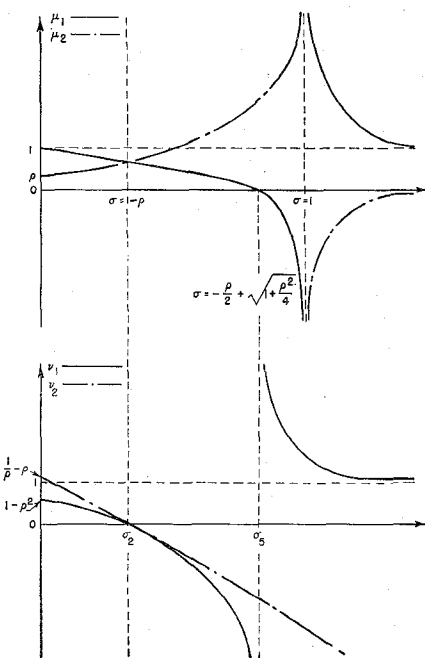


Fig. 4—Ferrite permeability parameters.

cated in Fig. 4. At the latter,  $\nu_1$  becomes infinite. At the former,  $\nu_1$  and  $\nu_2$  both become zero, their ratio remaining finite.

#### SURFACE WAVES AT A SINGLE INTERFACE

To obtain the secular equation determining the surface-wave propagation constants, we employ a transverse resonance procedure. For the structure in Fig. 3, this requires a knowledge of the admittances  $\overrightarrow{Y}_a$  and  $\overleftarrow{Y}_m$ . The former is simply the input admittance of an infinite transmission line for a  $TE_{n0}$  mode of an empty parallel plate waveguide. If we choose to normalize the fields so that the admittance for the TEM mode of this waveguide is unity, then  $\overrightarrow{Y}_a$  becomes

$$\overrightarrow{Y}_a = \frac{k_{xa}}{k} \quad (7)$$

We recall that the input admittance to an infinite modal transmission line corresponds to the ratio of the amplitudes of the transverse (to  $x$ ) magnetic and electric fields of that mode which propagates outward to infinity, *i.e.*, in this case, of the mode whose dependence on  $x$  is given by  $\exp(ik_{xa}x)$ . We obtain the admittance  $\overleftarrow{Y}_m$  via a similar requirement for the ferrite loaded waveguide. Thus, we define  $\overleftarrow{Y}_m$  as the ratio of the amplitudes of the transverse (to  $x$ ) magnetic and electric fields for a mode whose  $x$  dependence is  $\exp(-ik_{xm}x)$ . The admittance  $\overleftarrow{Y}_m$  is then obtained as<sup>1</sup>

$$\overleftarrow{Y} = \frac{k_{xm}}{kv_1} - i \frac{\kappa}{kv_2} \quad (8)$$

The secular equation is now obtained from the transverse resonance requirement

$$\vec{Y}_a + \vec{Y}_m = 0 = q_a + \frac{q_m}{\nu_1} - i \frac{\theta}{\nu_2} \quad (9)$$

where we have introduced the normalized wave numbers

$$q_a = \frac{k_{xa}}{k} \quad q_m = \frac{k_{xm}}{k} \quad \theta = \frac{\kappa}{k}. \quad (10)$$

As it stands, the secular equation (9) is ambiguous because of the quadratic nature of the relationships in (1). This ambiguity is resolved by recognizing that the fields of a surface-wave mode must decay exponentially away from the interface on both sides of the interface. Therefore, we require that  $\text{Im } q_a > 0$  and  $\text{Im } q_m > 0$ . Substitution from (1) into (9) now yields the following as the secular equation in terms of  $\theta$  only:

$$\sqrt{1 - \theta^2} + \frac{1}{\nu_1} \sqrt{\epsilon \nu_1 - \theta^2} - i \frac{\theta}{\nu_2} = 0$$

subject to

$$\begin{cases} \theta^2 > 1 & \text{Im } \sqrt{1 - \theta^2} > 0 \\ \theta^2 > \epsilon \nu_1 & \text{Im } \sqrt{\epsilon \nu_1 - \theta^2} > 0. \end{cases} \quad (11)$$

Since this is an algebraic equation, its solutions are readily obtained in closed form and are subject to exhaustive analysis. In the following, we give the results of such an analysis omitting most of the details of the required algebraic manipulations which, while complicated in detail, are quite straightforward.<sup>7,13</sup>

Solutions to (11) are obtained by squaring twice to obtain a quadratic equation in  $\theta^2$ . When  $\nu_1$  and  $\nu_2$  are eliminated via (6) the solution to this quadratic is obtained as

$$\theta_{\pm}^2 = \frac{1}{2\rho(u^2 - 1)} \left\{ (u^2 - 1)[\rho - (\epsilon - 1)u] + \frac{\rho^2}{4}(\epsilon + 1)u \right. \\ \left. \pm \sqrt{\left[ (u^2 - 1) - \frac{\rho^2}{4} \right] \left[ (\epsilon - 1)^2(u^2 - 1) - \frac{\rho^2}{4}(\epsilon + 1)^2 \right]} \right\} \quad (12)$$

where  $u = \frac{1}{2}\rho + \sigma$ . The plus or minus subscript associated with  $\theta^2$  distinguishes the solution with the corresponding algebraic sign preceding the radical (understood to be positive). Note that the solutions to the biquadratic given here do not necessarily provide solutions to (11). Such solutions result only when the restrictions indicated in (11) are satisfied. Moreover, when a particular  $\theta^2$  given by (12) does provide a solution to (11), it will satisfy the latter equation with only one or the other of  $\theta = \pm \sqrt{\theta^2}$ . Thus, the restrictions on the sign of the imaginary part of  $q_a$  and  $q_m$  serve to determine the algebraic sign of  $\theta$  appropriate to the particular solution.

A sketch of  $\theta_{\pm}^2$  as a function of  $\sigma$  with  $\rho$  held fixed is given in Fig. 5. We will now establish that only those values of  $\theta_{\pm}^2$  lying on the solid line segments of the

<sup>13</sup> A. D. Bresler, "TE<sub>00</sub> Surface Waves at Ferrite-Air Interfaces," Polytechnic Institute of Brooklyn, Brooklyn, N. Y., Microwave Research Institute, Memorandum R-723-59; February 28, 1959.

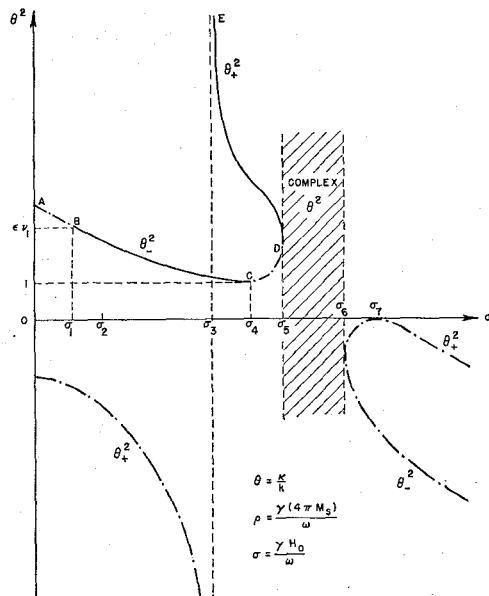
curves in Fig. 5 represent surface-wave solutions. In this discussion, we will make use of the information contained in the equations in Table I, where certain values of  $\sigma$  are distinguished and defined in terms of the fixed parameters  $\rho$  and  $\epsilon$ . It is readily verified that, for  $\rho > 0$  and  $\epsilon > 1$ ,  $\alpha > \beta$  implies  $\sigma_{\alpha} > \sigma_{\beta}$  except that  $\sigma_3$  may be  $\gtrless \sigma_4$ . Since the product of  $\rho$  and  $\sigma$  is always positive, it is sufficient to consider only  $\rho > 0$  and  $\sigma > 0$ . Note that if  $\rho$  and  $\sigma$  are both replaced by their negatives, *i.e.*, if the dc magnetic field is reversed, the only effect on the solutions indicated in (12) is to interchange  $\theta_+^2$  and  $\theta_-^2$ . The restriction to  $\rho > 0$ ,  $\sigma > 0$  means that if any  $\sigma_{\alpha}$  in Table I is found to be negative for  $\rho > 0$ , then that value of  $\sigma$  is no longer significant, *i.e.*, can no longer be obtained with the given ferrite at the given frequency.

From the information given in (12), Table I, and Fig. 5, it follows that surface-wave mode solutions may occur only in the interval  $0 < \sigma < \sigma_5$ . To justify this statement, we note that  $\theta_{\pm}^2$  are both equal to or less than zero for all  $\sigma > \sigma_6$  so that the restriction in (11) is not satisfied. In the interval  $\sigma_5 < \sigma < \sigma_6$ ,  $\theta_{\pm}^2$  are both complex. Surface-wave modes with complex propagation constants are not admissible. This is evident from the following considerations. If a complex  $\theta$  is a solution of (11) then its complex conjugate,  $\theta^*$ , must also be a solution. Suppose that the  $q_a$  and  $q_m$  associated with  $\theta$  are such that  $\text{Im } q_a > 0$  and  $\text{Im } q_m > 0$  so that  $\theta$  represents an admissible surface wave-mode. It follows that  $q_a^*$  and  $q_m^*$ , associated with  $\theta^*$ , are characterized by  $\text{Im } q_a^* < 0$  and  $\text{Im } q_m^* < 0$ . Therefore,  $\theta^*$  cannot be the propagation constant of an admissible surface-wave mode. It can be shown<sup>5</sup> that, in a dissipationless waveguide, complex modal propagation constants must occur in complex

conjugate pairs. Therefore, since we cannot admit  $\theta$  as a proper surface-wave solution and exclude  $\theta^*$ , we exclude all complex  $\theta$  from further consideration.

The outstanding feature to be observed in the range  $\sigma < \sigma_5$  is the infinite  $\theta_+^2$  solution which obtains for  $\sigma \rightarrow \sigma_3$ . This infinity is not associated with any peculiarity in the ferrite parameters since both  $\nu_{1,2}(\sigma_3)$  are finite and non-zero. Thus, this infinity might be described as a "waveguide resonance" as opposed to a "medium resonance."<sup>14</sup> Since a surface-wave solution must satisfy the restriction  $\theta^2 > 1$ , it follows that the infinite propagation

<sup>14</sup> The existence of this infinite solution in a ferrite slab loaded rectangular waveguide and its characterization as a "waveguide resonance" is noted by H. Seidel in ref. 1. Seidel gives the condition for the existence of this resonance as  $\omega_2 = \frac{1}{2}\gamma(B_0 + H_0)$  where  $B_0 = H_0 + 4\pi M_s$ . This is exactly equivalent to  $\sigma_3 = 1 - \frac{1}{2}\rho$ . For the benefit of readers more familiar with descriptions of critical points in terms of  $B_0$  and  $H_0$  we take this opportunity to point out that  $\sigma_2$  and  $\sigma_5$  are exactly equivalent to  $\omega_2 = \gamma B_0$  and  $\omega_5 = \gamma \sqrt{B_0 H_0}$ , respectively.

Fig. 5— $\theta_{\pm}^2$  as a function of  $\sigma$  with  $\rho$  fixed.

constant at  $\sigma_3$  may be associated with a surface-wave solution only for  $\sigma \rightarrow \sigma_3$  from above. It is readily demonstrated that  $\theta_+^2$  has only the single zero shown in Fig.

5 at  $\sigma_7$  and that  $\theta_-^2$  has no zeros. In Table I it is indicated that  $\theta_-^2$  passes through a minimum at  $\sigma_4$  and that its value there is always one. With this information, we conclude that surface-wave solutions may occur only on the curve passing through the points labeled A through E in Fig. 5.

We now assert that surface-wave mode solutions are obtained only on the segments BC and DE (the solid line segments) of the curve in Fig. 5. Moreover, we assert that  $\theta_-^2$  on BC represents a solution such that  $\theta_- > 1$  whereas  $\theta_+^2$  on DE represents a solution such that  $\theta_+ < -1$ . In the following, we will give only a brief outline of the analysis required to justify these assertions.<sup>13</sup> To facilitate the discussion which follows we rewrite (11) as

$$\theta = \nu_2 \sqrt{\theta^2 - 1} + \frac{\nu_2}{\nu_1} \sqrt{\theta^2 - \epsilon \nu_1} . \quad (13)$$

The "admissible" solutions of this equation must, of course, still satisfy the restrictions  $\theta^2 > 1$  and  $\theta^2 > \epsilon \nu_1$ . This version of the secular equation makes evident that only one of the two square roots of either  $\theta_+^2$  or  $\theta_-^2$  may be an admissible surface-wave solution. Now, in the interval  $0 < \sigma < \sigma_5$ ,  $\theta_-^2$  is a single valued continuous func-

TABLE I

$\sigma$	$\theta_{\pm}^2$	$\nu_1$	$\nu_2$
$\sigma = 0$	$\theta_{\pm}^2 = \frac{(\epsilon - 3)\rho + \rho^3 \pm 2\sqrt{(\epsilon - 1)^2 + \epsilon\rho^2}}{\rho(\rho^2 - 4)}$	$1 - \rho^2$	$\frac{1}{\rho} - \rho$
$\sigma_1 \approx -\rho + \sqrt{1 - \rho} \sqrt{\frac{\epsilon}{\epsilon - 1}} \quad \left( \frac{\rho}{\epsilon - 1} \ll \frac{\epsilon\rho^2}{\epsilon + 1} < 1 \right)$	$\theta_-^2 = \epsilon \nu_1 \approx \frac{\epsilon \sqrt{\epsilon}}{\sqrt{\epsilon} + \sqrt{(\epsilon - 1) - \rho \sqrt{\epsilon(\epsilon - 1)}}} > 1$	$\nu_1 > \frac{1}{\epsilon}$	$\nu_2 > \frac{1}{\epsilon}$
$\sigma_2 = 1 - \rho$	$\theta_{\pm}^2 = \frac{2(\epsilon - 1) - \epsilon\rho \pm 2\sqrt{(\epsilon - 1)^2 + \epsilon\rho}}{\rho(\rho - 4)}$	0	0
$\sigma_3 = 1 - \frac{\rho}{2}$	$\theta_+^2 = \infty$ $\theta_-^2 = \left[ \frac{4 + (\epsilon + 1)\rho}{2\sqrt{4(\epsilon + 1)\rho}} \right]^2 \geq 1$	$-\frac{4 + \rho}{\rho}$	$-\frac{4 + \rho}{4}$
$\sigma_4 = -\frac{\epsilon}{\epsilon - 1} \cdot \frac{\rho}{2} + \sqrt{1 + \frac{1}{4} \left( \frac{\epsilon\rho}{\epsilon - 1} \right)^2}$	$\theta_-^2 = 1 \quad \left( \frac{d}{d\sigma} \theta_-^2 = 0 \right)$		
$\sigma_5 = -\frac{\rho}{2} + \sqrt{1 + \frac{\rho^2}{4}}$	$\theta_+^2 = \theta_-^2 = \frac{1}{2} + \sqrt{\frac{1}{4} + \frac{1}{\rho^2}} \geq 1$	$\infty$	$-\frac{\rho}{2} - \sqrt{1 + \frac{\rho^2}{4}}$
$\sigma_6 = -\frac{\rho}{2} + \sqrt{1 + \left( \frac{\epsilon + 1}{\epsilon - 1} \cdot \frac{\rho}{2} \right)^2}$	$\theta_+^2 = \theta_-^2 = \frac{1}{2} - \sqrt{\frac{1}{4} + \frac{1}{\rho^2} \left( \frac{\epsilon - 1}{\epsilon + 1} \right)^2} \leq 0$		
$\sigma_7 = -\frac{\epsilon - 2}{\epsilon - 1} \cdot \frac{\rho}{2} + \sqrt{1 + \frac{1}{4} \left( \frac{\epsilon\rho}{\epsilon - 1} \right)^2}$	$\theta_+^2 = 0 \quad \left( \frac{d}{d\sigma} \theta_+^2 = 0 \right)$	$\epsilon$	

tion of  $\sigma$ . Therefore, if  $\theta_-$ , one of the square roots of  $\theta_-^2$ , is a proper solution of (13) in one part of this interval but not in another part, the change must occur either where  $\theta_-^2=1$  (at point *C*) or where  $\theta_-^2=\epsilon\nu_1$  (at point *B*). In the interval  $\sigma_3 < \sigma < \sigma_5$ ,  $\theta_+^2$  is also a single-valued continuous function of  $\sigma$  and, moreover, is always greater than both 1 and  $\epsilon\nu_1$  in this interval. Therefore, if one of the square roots of  $\theta_+^2$  provides a proper surface-wave solution at any point of the segment *DE*, it must provide a proper solution at all points of this segment. Finally, we observe that if  $\theta(\sigma)$  represents a proper surface-wave solution in some continuous interval in  $\sigma$  then either  $\theta > 1$  or  $\theta < -1$  throughout this interval. With these observations, the significance of the successive steps in the analysis outlined in the next paragraph should be evident.

The first step in the analysis is to consider the behavior of (13) in the limit as  $\theta_+^2 \rightarrow \infty$ . If  $\nu_1$  and  $\nu_2$  are eliminated from (13) by substituting their known values at  $\sigma_3$ , given in Table I, it becomes evident that, for  $\theta_+^2 \rightarrow \infty$ ,  $\theta_+ \rightarrow -\infty$  is a proper surface-wave solution near point *E* (*i.e.*, as  $\sigma \rightarrow \sigma_3$  from above). It then follows that  $\theta_+ < -1$  must be a proper surface-wave solution throughout the segment *DE*. An independent verification of this conclusion may be obtained by demonstrating that, in the neighborhood of point *D*, points on *DE* are proper solutions with  $\theta_+ < -1$ , whereas points on *CD* are not proper solutions. This implies that surface-wave solutions do not exist on the segment *CD*. The next step in the analysis is to show that  $\theta_-(\sigma_3) > 1$  is a proper surface-wave solution if and only if  $(\epsilon+1)\rho > 4$ . Since  $\sigma_4 \gtrless \sigma_3$  according as  $(\epsilon+1)\rho \gtrless 4$ , this verifies the conclusion that points on *CD* do not represent proper solutions. In addition, it shows that points on *BC*, with  $\theta_- > 1$ , do represent admissible surface-wave mode solutions. Point *B* is defined by the requirement that  $\theta_-^2(\sigma_1) = \epsilon\nu_1(\sigma_1)$ . This requirement is satisfied with  $\sigma_1 > 0$  for all  $\rho$  less than some upper bound. For sufficiently large  $\epsilon$ , in particular, for the range of  $\epsilon$  values characteristic of most ferrites, the upper bound is given by  $\rho_u \approx 0.6$ . Thus, the final step in the analysis is to show that  $\theta_-^2(0)$  does not provide a proper surface-wave solution when  $\rho$  is sufficiently small. From this we conclude that, when  $\sigma_1 > 0$ , points on *AB* do not represent proper surface-wave mode solutions.

The conclusions we have drawn from the analysis described above are summarized in Fig. 6(a) where we indicate the behavior of the surface-wave mode propagation constants as a function of  $\sigma$ , *i.e.*, as a function of the dc magnetic field at a fixed frequency. To obtain analogous results applicable when the dc magnetic field is fixed and the frequency is varied, we introduce the variables

$$\Omega = \frac{1}{\sigma} = \frac{\omega}{\gamma H_0}, \quad m = 1 + \frac{\rho}{\sigma} = 1 + \frac{4\pi M_s}{H_0} \geq 1 \quad (14)$$

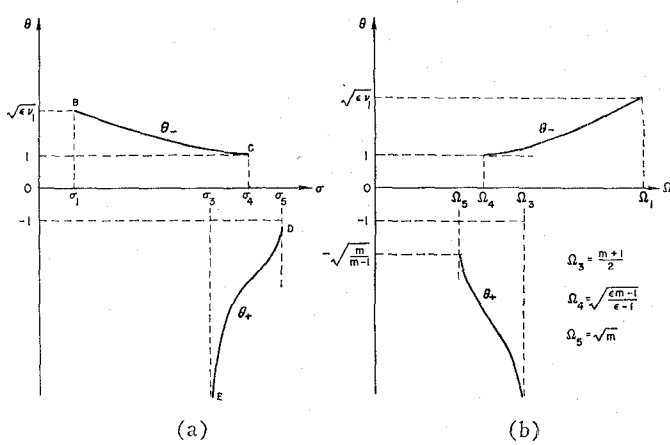


Fig. 6—Surface wave propagation constants. (a)  $\rho = \text{constant}$ ,  $\omega = \text{constant}$ ,  $\sigma \sim H_0$ . (b)  $H_0 = \text{constant}$ ,  $m = 1 + \rho/\sigma = \text{constant}$ ,  $\Omega = 1/\sigma \sim \omega$ .

where  $m$  is independent of frequency and, for fixed  $H_0$ ,  $\Omega$  is directly proportional to the frequency. Expressions for  $\nu_{1,2}$  as functions of  $\Omega$  and  $m$  instead of  $\rho$  and  $\sigma$  are readily obtained and the entire analysis may be repeated. Most of the required information can be obtained by direct substitution into the result of the earlier analysis and a reinterpretation of these results for  $m$  fixed and  $\Omega$  as the variable. The results of this new analysis are shown in Fig. 6(b). The surface-wave cutoff points  $\Omega_{3,4,5}$  are defined there in terms of  $m$  and  $\epsilon$ . For  $\epsilon > 1$  and  $m > 1$ , all these cutoff points are finite and non-zero. The two frequency ranges in which surface waves are permitted will overlap, *i.e.*,  $\Omega_3 > \Omega_4$ , when  $(\epsilon-1)m > (\epsilon+3)$ . In the earlier analysis, the low-field cutoff point  $\sigma_1$  was obtained from the solution of a quartic equation. The expression for  $\sigma_1$  given in Table I is an approximate solution of this quartic valid subject to the assumptions indicated in Table I in connection with the expression for  $\sigma_1$ . In the present analysis, it is possible to obtain an exact expression for  $\Omega_1$  since the quartic equation for  $\sigma_1$  transforms to a quadratic equation in  $\Omega_1^2$ . The solution of this biquadratic which corresponds to the requirement  $\theta_-^2 = \epsilon\nu_1$  is

$$\Omega_1^2 = \frac{\alpha + \sqrt{\alpha^2 - 4(\epsilon-1)(\epsilon m - 1)m^3}}{2(\epsilon-1)}$$

where

$$\alpha = (3\epsilon-1)m^2 - (2\epsilon+1)m + \epsilon. \quad (15)$$

For all  $\epsilon > 1$ ,  $\Omega_1^2$  is finite so that this high-frequency cutoff point always occurs. This is consistent with the results of our earlier analysis since, for any ferrite,  $\rho$  approaches zero as  $\omega$  goes to infinity.

Fig. 7 shows computed curves of  $\theta$  as a function of  $\sigma$  for values of  $\rho$  and  $\epsilon$  chosen to cover the range of values characteristic of most ferrites at *X* band.<sup>15</sup> Note that an

<sup>15</sup> S. Sensiper, "Resonance loss properties of ferrites in the 9-kmc region," PROC. IRE, vol. 44, pp. 1323-1342; October, 1956.

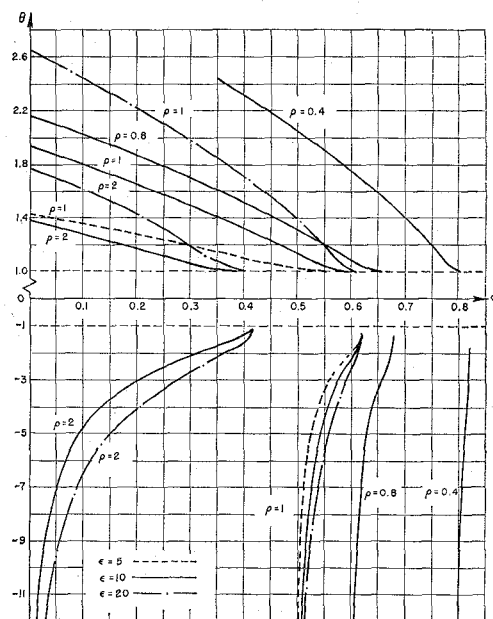


Fig. 7—Propagation constants for surface waves at a ferrite-air interface (for fixed frequency).

expanded scale has been employed for  $\theta > 1$ . The curves in Fig. 7 make it evident that, for fixed  $\rho$  and  $\sigma$ ,  $|\theta|$  increases with increasing  $\epsilon$  and that, for  $\epsilon$  and  $\sigma$  fixed,  $|\theta|$  decreases with increasing  $\rho$ . The only positive directed ( $\theta > 1$ ) surface wave which exhibits a low-field cutoff point is that for  $\rho = 0.4$ . This is consistent with the requirement indicated earlier that  $\rho$  be less than approximately 0.6 for this cutoff point to make its appearance.

To conclude this section, we note that we have shown that two oppositely directed  $TE_{n0}$  surface-wave modes are guided along a plane interface separating a dissipationless anisotropic (transversely magnetized) ferrite from free space. The two surface waves exist in different finite ranges of the parameter values. These two ranges never coincide and may or may not overlap. In contrast to the behavior of more familiar surface-wave phenomena, the surface waves here under consideration always exhibit both high- and low-frequency cutoff points (for fixed dc magnetic field). In addition, at a fixed frequency, each of the two surface waves cuts off for sufficiently high dc magnetic field and may or may not (depending on the parameter values) also cut off for sufficiently low dc magnetic field. The propagation constant of one of the two surface waves becomes infinite at the low-field (high-frequency) cutoff point. The behavior of this infinite propagation constant, when the guiding surface is located in different environments, will be the major subject of discussion in the next section.

## SURFACE WAVES ON FERRITE SLABS

In this section we will be concerned with the  $TE_{n0}$  surface waves guided along finite thickness ferrite slabs located as indicated in Fig. 8. The secular equations determining the surface-wave propagation constants are again obtained via the transverse resonance procedure described above. For this purpose we employ, in addi-

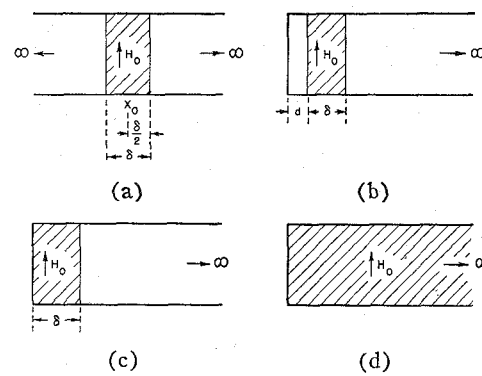


Fig. 8—Ferrite loaded parallel plate waveguides. (a) Ferrite slab in free space. (b) Ferrite slab near a short circuit. (c) Ferrite slab at a short circuit. (d) Ferrite filled semi-infinite waveguide.

tion to the admittances defined in (7) and (8), the impedance transfer formulas given by Morgenthaler<sup>16</sup> for  $TE_{n0}$  modes in ferrite media. We will be interested primarily in the surface-wave solutions with large  $\theta$ . With this in mind we let

$$q_a = iQ_a \quad q_m = iQ_m. \quad (16)$$

From (1) and (10) it follows that the wave numbers  $\theta$ ,  $Q_a$ , and  $Q_m$  are related through

$$\theta^2 = 1 + Q_a^2 = \epsilon \nu_1 + Q_m^2. \quad (17)$$

Thus, for finite  $\nu_1$ ,  $\theta^2 \rightarrow \infty$  implies  $Q_a^2 \rightarrow \infty$  and  $Q_m^2 \rightarrow \infty$ . For each of the structures in Fig. 8(a), (b), (c) the empty region extends to infinity. We must therefore require that  $Q_a > 0$ .

Before writing down the secular equation for the ferrite slab in free space [see Fig. 8(a)], it is instructive to predict some of the features of this equation. Suppose we choose to write the transverse resonance equation in terms of the admittances at  $x_0$ , the midpoint of the slab. With this choice, the total admittance is given as the sum of the admittances  $\overrightarrow{Y}(x_0; H_0)$  and  $\overleftarrow{Y}(x_0; H_0) = \overrightarrow{Y}(x_0; -H_0)$ . Thus, while each of these admittances depends on the direction of  $H_0$ , their sum is independent of this direction. We therefore expect that the secular equation will be an even function of  $\nu_2^2$ . Also, since reversing the direction of  $H_0$  is equivalent to a  $180^\circ$  rotation about the  $x$  axis, the secular equation must contain only even powers of  $\theta$ . These requirements are evidently satisfied by the secular equation

$$Q_a^2 + \frac{2Q_aQ_m}{\nu_1} \coth k\delta Q_m + \frac{Q_m^2}{\nu_1^2} - \frac{\theta^2}{\nu_2^2} = 0. \quad (18)$$

For a sufficiently thick slab, *i.e.*, for  $k\delta Q_m$  sufficiently large, the two interfaces should behave independently. That this is the case is verified by noting that in the thick slab limit (18) becomes

<sup>16</sup> F. R. Morgenthaler, "Transverse impedance transformation for ferromagnetic media," PROC. IRE, vol. 45, p. 1407; October, 1957. The time dependence assumed in this reference is  $\exp(j\omega t)$  not, as in this paper,  $\exp(-j\omega t)$ . Note that the term following the plus sign in the numerator of the right hand side of (4) of this reference has been omitted. The omitted term is simply the quantity  $j$ .

$$\left( Q_a + \frac{Q_m}{\nu_1} + \frac{\theta}{\nu_2} \right) \left( Q_a + \frac{Q_m}{\nu_1} - \frac{\theta}{\nu_2} \right) = 0. \quad (19)$$

This equation shows clearly that each interface of a thick slab supports a pair of surface waves whose propagation constants are either those in Fig. 6 (for the interface at  $x = \frac{1}{2}\delta$ ) or the negatives of those in Fig. 6. With certain minor modifications,<sup>13</sup> this conclusion is valid for any slab thickness throughout most of the range in which the surface waves propagate. The conclusions noted above are summarized in the sketches in Fig. 9. Note that the curves labeled *RH* in Fig. 9 are practically identical with those in Fig. 6(a) except in the immediate vicinity of  $\sigma_5$ . Note also that the low-field cutoff point  $(\sigma_1')$  indicated in Fig. 9 is not simply related to the corresponding point  $(\sigma_1)$  in Fig. 6(a).

The behavior of the infinite propagation constants will play a significant role in the discussions which follow. For this reason, it is pertinent to establish that, for any slab thickness,  $\theta$  approaching both  $\pm\infty$  are proper solutions of (18) for  $\sigma \rightarrow \sigma_3$  from above. We recall that  $\nu_1$  is finite in the neighborhood of  $\sigma_3$  and therefore  $\theta^2 \rightarrow \infty$  implies  $\theta^2 \approx Q_a^2 \approx Q_m^2 \rightarrow \infty$ . Thus, for  $\theta$  approaching either  $\pm\infty$ , (18) may be approximated by

$$\coth k\delta|\theta| = -\frac{\nu_1}{2} \left( 1 + \frac{1}{\nu_1^2} - \frac{1}{\nu_2^2} \right) = h(\sigma) \quad (20)$$

where, since  $Q_a$  must be positive, we have replaced  $Q_a$  by  $|\theta|$  and, since  $Q_m \coth k\delta Q_m > 0$  for  $Q_m \gtrless 0$ , we have replaced this term by  $|\theta| \coth k\delta|\theta|$ . Therefore,  $\theta \rightarrow \pm\infty$  are both allowed solutions when  $h(\sigma) \rightarrow 1$  from above or, as is evident from Fig. 10(a), as  $\sigma \rightarrow \sigma_3$  from above.

In turning now to the analysis of the structure in Fig. 8(b) we are, in effect, asking the following question. What is the effect on the surface waves guided along a ferrite slab of locating one side of the slab near a short circuit? So long as we are interested only in the region in which  $|\theta|$  is very large, the answer must be that the short circuit will have very little effect since the surface waves are very tightly bound to the two interfaces. In particular, we certainly expect that for any  $d \neq 0$  the surface-wave propagation constants must still approach both  $\pm\infty$  as  $\sigma \rightarrow \sigma_3$  from above. To verify that this is indeed the case, we employ the transverse resonance procedure described earlier to obtain

$$Q_a^2 \coth kdQ_a + (1 + \coth kdQ_a) \frac{Q_a Q_m}{\nu_1} \coth k\delta Q_m + (1 - \coth kdQ_a) \frac{Q_a \theta}{\nu_2} + \frac{Q_m^2}{\nu_1^2} - \frac{\theta^2}{\nu_2^2} = 0 \quad (21)$$

as the secular equation for the waveguide shown in Fig. 8(b). It is immediately evident that as  $Q_a \rightarrow \infty$  with  $d \neq 0$  this equation reduces to (18). This verifies the assertion made above concerning the infinite solutions to (21) in the neighborhood of  $\sigma_3$ . Suppose now that the right hand interface of the structure in Fig. 8(b) is al-

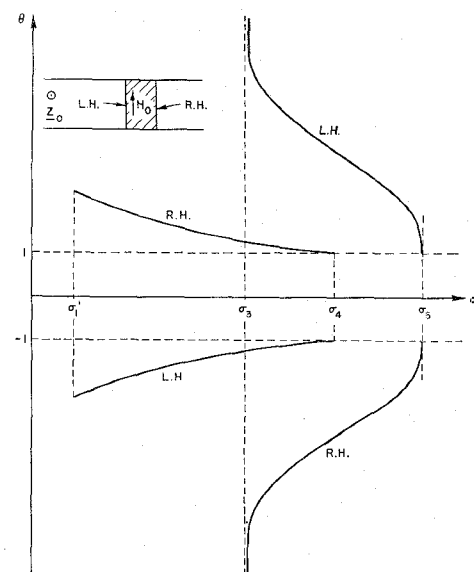


Fig. 9—Propagation constants for surface waves on a ferrite slab in free space.

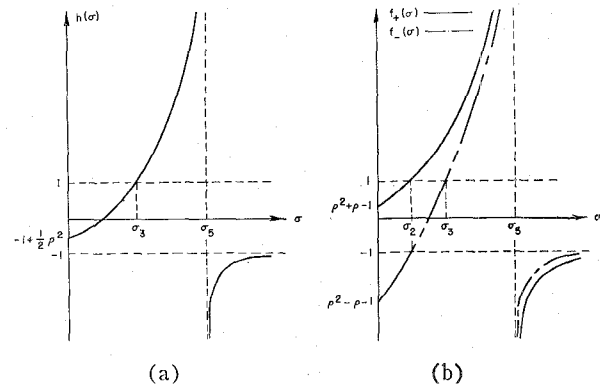


Fig. 10—The functions of  $h(\sigma)$  and  $f_{\pm}(\sigma)$ .

$$(a) h(\sigma) = -1 + \frac{1}{2} \frac{\rho^2}{1 - \sigma(\rho + \sigma)} \quad (b) f_{\pm}(\sigma) = \frac{(\rho + \sigma)^2 \pm \rho - 1}{1 - \sigma(\rho + \sigma)}.$$

lowed to recede to infinity. The surface waves which the resulting structure would support would be those of the left-hand interface modified by the presence of the short circuit. It is evident that in this case we would find, for any  $d \neq 0$ , that there still exists an infinite solution ( $\theta \rightarrow +\infty$  only) as  $\sigma \rightarrow \sigma_3$  from above. On the other hand, if we set  $d = 0$  and so obtain the structure in Fig. 8(d) the surface waves must vanish completely since, as can readily be shown,<sup>13</sup> this structure will not support a surface wave. The discontinuous behavior noted here implies that a similar discontinuous behavior will be found in the comparison of the behavior of the surface waves for the structures in Figs. 8(b) and 8(c).

When the ferrite slab is against the short circuit [see Fig. 8(c)], the secular equation is obtained by setting  $d = 0$  in (21). This yields<sup>2,17</sup>

<sup>17</sup> R. L. Pease, "On the propagation of surface waves over an infinite grounded ferrite slab," IRE TRANS. ON ANTENNAS AND PROPAGATION, vol. 6, pp. 13-21; January, 1958. Pease discusses the solutions to this equation in the thin slab approximation.

$$Q_a + \frac{Q_m}{\nu_1} \coth k\delta Q_m - \frac{\theta}{\nu_2} = 0. \quad (22)$$

To investigate the infinite solutions of this equation, we proceed as we did in connection with (20) and, for  $|\theta| \rightarrow \infty$ , approximate this equation by

$$\coth k\delta |\theta| = \pm \frac{\nu_1}{\nu_2} - \nu_1 = f_{\pm}(\sigma) \quad (\theta \rightarrow \pm \infty). \quad (23)$$

The  $\pm$  sign which appears in this equation (associated with  $\theta \rightarrow \pm \infty$ ) results from replacing  $\theta$  by  $\pm |\theta|$  according as  $\theta \gtrless 0$ . It is evident from (23) that  $\theta \rightarrow \pm \infty$  are allowed solutions of (22) only for  $f_{\pm}(\sigma) \rightarrow 1$  from above. Sketches of these two functions are shown in Fig. 10(b). An examination of these sketches makes evident that  $\theta \rightarrow \infty$  will be a solution for  $\sigma \rightarrow \sigma_2$  from above whereas the solution  $\theta \rightarrow -\infty$  occurs, as before, for  $\sigma \rightarrow \sigma_3$  from above.

We have now arrived at the major result of this section. We saw earlier that when the ferrite slab was arbitrarily close to but not at the short circuit, *i.e.*, in the limit as  $d \rightarrow 0$ , there were two infinite solutions allowed, both occurring for  $\sigma \rightarrow \sigma_3$  from above. These two infinite solutions are shown in Fig. 11(a). On the other hand, when the ferrite slab is at the short circuit, *i.e.*, at the limit  $d = 0$ , there are still two infinite solutions, but the  $\theta \rightarrow +\infty$  solution is suddenly found at  $\sigma \rightarrow \sigma_2$  from above instead of  $\sigma \rightarrow \sigma_3$  from above. The two infinite solutions in this case are shown in Fig. 11(b). The discontinuous behavior of the  $\theta \rightarrow +\infty$  solution is evident from a comparison of Fig. 11(a) and (b). This discontinuous behavior will play a significant role in the discussions which follow.

#### THE $TE_{n0}$ PROPAGATING MODES OF THE SLAB LOADED RECTANGULAR WAVEGUIDE

The secular equation determining the propagation constants of the  $TE_{n0}$  modes of the waveguide in Fig. 1 is<sup>2,16</sup>

$$q_a \cot K(1 - \Delta)q_a + \frac{q_m}{\nu_1} \cot K\Delta q_m - \frac{\theta}{\nu_2} = 0 \quad (24)$$

where the dimensionless parameters  $K$  and  $\Delta$  are defined as

$$K = ka = 2\pi \frac{a}{\lambda}; \quad \Delta = \frac{\delta}{a} \quad (0 \leq \Delta \leq 1). \quad (25)$$

For the propagating modes,  $\theta$  is real while  $q_{a,m}$  may be either real or imaginary. Since the secular equation is an even function of both  $q_a$  and  $q_m$  we may, without loss of generality, prescribe that these be positive when they are real and that  $\text{Im } q_a, q_m > 0$  when they are imaginary.

Very little has been published concerning the complete set of propagating mode solutions of (24). Some data has been given for a few special choices of the parameter values.<sup>2</sup> In addition, for thin slabs, perturbation

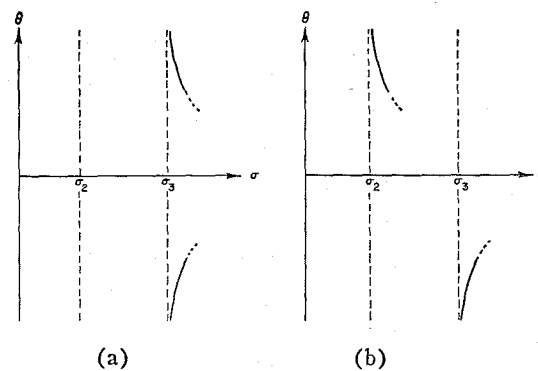


Fig. 11—Infinite propagation constants for surface waves on a ferrite slab near a short circuit. (a)  $d \rightarrow 0$ . (b)  $d = 0$ .

formulas are available<sup>15,18</sup> in which the solutions to (24) are obtained as first-order perturbations about the propagation constants of the empty waveguide.

The analysis which follows is confined to the behavior of the propagation constants at a fixed frequency as a function of the dc magnetic field and the normalized slab thickness. It is convenient to assume that this fixed frequency is such that  $\pi < K < 2\pi$ , *i.e.*, such that the empty waveguide propagates only the  $TE_{10}$  mode. It will become evident as we proceed that this does not seriously restrict the generality of the conclusions we will draw.

Since the secular equation (24) is transcendental, we cannot obtain its solutions in closed form. The results presented below were obtained by a combination of analytical and graphical investigations, the details of which are given elsewhere.<sup>7</sup> In the following, the discussion will be primarily descriptive rather than deductive.

The propagating  $TE_{n0}$  modes of the waveguide in Fig. 1 are of two kinds, a "surface-wave mode" bound to the interface at  $x = \delta$  and the "ordinary waveguide modes." The latter are the modes whose properties can be understood (except for the effect of the ferrite anisotropy) by assigning to the ferrite slab an equivalent dielectric constant of  $\epsilon\nu_1$ . We expect that, except for  $\Delta \rightarrow 1$ , the characteristics of the surface-wave mode will be very similar to those described earlier for the waveguide in Fig. 8(c). It is therefore not surprising that, by following the procedure employed in connection with (23), we again find that for  $\theta^2 > \epsilon\nu_1$  (so that  $q_a$  and  $q_m$  are both imaginary for  $\theta^2 \rightarrow \infty$ ) there are precisely two infinite  $\theta$  solutions and that these occur as follows: (a)  $\theta \rightarrow +\infty$  as  $\sigma \rightarrow \sigma_2$  from above; (b)  $\theta \rightarrow -\infty$  as  $\sigma \rightarrow \sigma_3$  from above.

To justify the statement that  $\epsilon\nu_1$  plays the role of an effective dielectric constant in determining the properties of the ordinary waveguide modes, we point out, first, that the relationship between  $\theta^2$  and  $q_m^2$  involves only  $\epsilon\nu_1$ . Further, we note that the modal propagation

<sup>18</sup> B. Lax, K. J. Button, and L. M. Roth, "Ferrite phase shifters in rectangular waveguide," *J. Appl. Phys.*, vol. 25, pp. 1413-1421; November, 1954.

constants for the completely filled ferrite loaded waveguide (*i.e.*, for  $\Delta=1$ ) are given by<sup>19</sup>

$$\theta = \pm \sqrt{\epsilon\nu_1 - \left(\frac{n\pi}{K}\right)^2} \quad n = 1, 2, 3, \dots \quad (26)$$

Finally, we note that the only place in which  $\nu_2$  has appeared so far is in the linear term in  $\theta$  in the secular equation (24). In the isotropic limit, *i.e.*, for  $\nu_2 \rightarrow \infty$ , this secular equation reduces to one which is very similar to the one which would apply for a dielectric slab with dielectric constant  $\epsilon\nu_1$ . Now, for  $\pi < K < 2\pi$ , the empty waveguide ( $\Delta=0$ ) propagates only a single pair of modes (two  $TE_{10}$  modes, one in each direction along  $z$ ). It is evident from (26) that the number of pairs of modes propagated by the completely filled waveguide depends on  $\epsilon\nu_1$ . For  $\nu_1 < 0$ , no modes may propagate, and therefore increasing the slab thickness will tend to cut off the modes which propagate at  $\Delta=0$ . This will also be true for  $\nu_1 > 0$ , but  $\epsilon\nu_1 < (\pi/K)^2$ . On the other hand, for  $\epsilon\nu_1$  positive and large, the completely filled waveguide will propagate many pairs of modes and therefore increasing the slab thickness should have the tendency to increase the number of propagating modes. We recall that  $\nu_1$  approaches infinity in the neighborhood of  $\sigma_5$ . From the remarks above, we conclude that, except for the surface-wave mode, the slab loaded waveguide must become completely cut off as  $\nu_1 \rightarrow -\infty$ , *i.e.*, as  $\sigma \rightarrow \sigma_5$  from below. On the other hand, we expect to find a large number of propagating modes for  $\nu_1 \rightarrow +\infty$ , *i.e.*, as  $\sigma \rightarrow \sigma_5$  from above.

It was noted earlier that, subject to the restriction  $\theta^2 > \epsilon\nu_1$ , there are precisely two infinite  $\theta$  solutions to (24). The indicated restriction need not apply when  $\nu_1 \rightarrow +\infty$ . Suppose then we assume that  $\nu_1$  and  $\theta^2$  are both large, but such that  $\epsilon\nu_1 - \theta^2 > 0$ . In this case, for  $\Delta \neq 0$  and  $\Delta \neq 1$ , we may approximate (24) by

$$\left(1 \mp \frac{1}{\nu_2}\right)|\theta| + \frac{1}{\nu_1} \sqrt{\epsilon\nu_1 - \theta^2} \cot K\Delta \sqrt{\epsilon\nu_1 - \theta^2} = 0 \quad (\theta \gtrless 0). \quad (27)$$

This equation is satisfied by many (large) values of  $\theta$ , both positive and negative. The solutions are located approximately at the poles of the cotangent function. Finally, in the limit as  $\nu_1 \rightarrow \infty$ ,  $\theta^2 \rightarrow \infty$ , subject to  $\epsilon\nu_1 - \theta^2 > 0$ , we find an infinity of positive and negative infinite solutions for  $\theta$ . These solutions represent surface waves which are bound to the ferrite-air interface on the air side only. The existence of such surface waves was ignored in the discussions above since these were concerned with surface waves which could exist on a single isolated interface. Since we have now determined the admitted infinite  $\theta$  solutions for both  $\theta^2 > \epsilon\nu_1$  and  $\theta^2 < \epsilon\nu_1$

(with  $\Delta=0$  and  $\Delta=1$ ), these must constitute the complete set of infinite solutions.

The restrictions  $\Delta \neq 0$  and  $\Delta \neq 1$ , noted in the preceding paragraph, do not represent a meaningless quibble. To see why this is so we note that the surface-wave modes cannot exist for either  $\Delta=0$  or  $\Delta=1$ . How does the surface wave mode disappear as  $\Delta \rightarrow 0$  and  $\Delta \rightarrow 1$ ? One way in which this can be accomplished is to have the surface-wave mode disappear via  $\theta^2 \rightarrow \infty$ . To investigate this possibility, we note that when  $|\theta| \rightarrow \infty$  and  $\Delta \rightarrow 0$  (the product  $|\theta|$  remaining finite and nonzero) the secular equation (24) may be approximated by

$$\coth K\Delta|\theta| = \pm \frac{\nu_1}{\nu_2} - \nu_1 = f_{\pm}(\sigma) \quad (\theta \gtrless 0). \quad (28)$$

Similarly, when  $|\theta| \rightarrow \infty$  and  $\Delta \rightarrow 1$  (the product  $[1-\Delta]|\theta|$  remaining finite and non-zero), the secular equation (24) may be approximated by

$$\coth K(1-\Delta)|\theta| = \pm \frac{1}{\nu_2} - \frac{1}{\nu_1} = g_{\pm}(\sigma) \quad (\theta \gtrless 0). \quad (29)$$

We therefore conclude that, for  $\Delta \rightarrow 0$ , infinite solutions for  $\theta$  exist only when  $f_{\pm}(\sigma) \geq 1$  while, for  $\Delta \rightarrow 1$ , such solutions are admitted only when  $g_{\pm}(\sigma) \geq 1$ . Examination of Figs. 10(b) and 12 makes evident that the infinite solutions under consideration can occur only as follows:

$$\begin{array}{lll} \text{range of } \sigma & \sigma_2 < \sigma < \sigma_3 & \sigma_3 < \sigma < \sigma_5 \\ \text{for } \Delta \rightarrow 0 & \theta \rightarrow +\infty & \theta \rightarrow \pm\infty \\ \text{for } \Delta \rightarrow 1 & \theta \rightarrow -\infty & \text{no infinities.} \end{array} \quad (30)$$

The next step in the analysis is concerned with the determination of the conditions for cutoff. For  $\theta=0$ , the secular equation (24) becomes

$$\cot K(1-\Delta) + \frac{\sqrt{\epsilon\nu_1}}{\nu_1} \cot K\Delta \sqrt{\epsilon\nu_1} = 0. \quad (31)$$

The values of  $\nu_1$  required for cutoff are readily determined at those values of  $\Delta$  for which  $\cot K(1-\Delta)$  is either zero or infinite as follows:

for  $\Delta = 1 - m\pi/K$ ,

$$\nu_1 = \frac{n^2}{\epsilon} \left( \frac{K}{\pi} - m \right)^{-2};$$

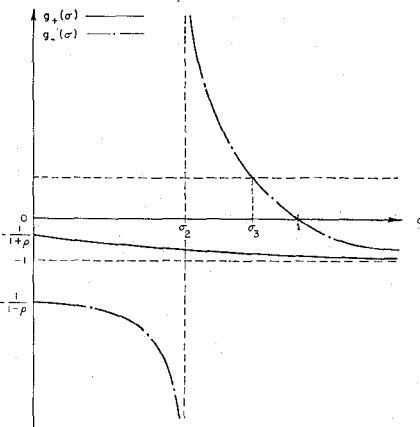
for  $\Delta = 1 - (2m+1)\pi/2K$ ,

$$\nu_1 = \frac{(2n+1)^2}{4\epsilon} \left( \frac{K}{\pi} - \frac{2m+1}{2} \right)^{-2} \text{ and } \nu_1 \rightarrow -\infty. \quad (32)$$

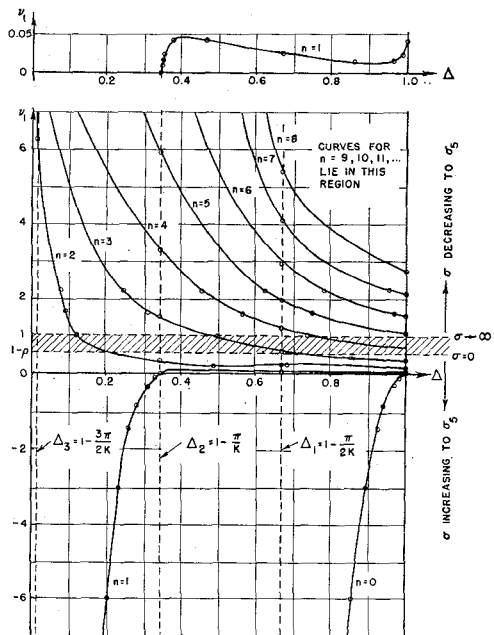
In each case,  $m=0, 1, 2, \dots$  up to the largest integer for which  $\Delta \geq 0$  and  $n=0, 1, 2, \dots$ . Fig. 13 shows sketches of the values of  $\nu_1$  at cutoff as a function of  $\Delta$  for  $K=1.52\pi$  and  $\epsilon=10$ .<sup>20</sup> Points which were actually

<sup>19</sup> P. S. Epstein, "Theory of wave propagation in a gyromagnetic medium," *Rev. Mod. Phys.*, vol. 28, pp. 3-17; January, 1956.

<sup>20</sup> The value chosen for  $K$  is appropriate for, RG 52/U rectangular waveguide (inner dimensions 0.4 inch  $\times$  0.9 inch) at 10 kmc.

Fig. 12—The functions  $g_{\pm}(\sigma)$ .

$$g_{\pm}(\sigma) = \pm \frac{1}{v_2} - \frac{1}{v_1} = - \frac{(\sigma \pm 1)(\rho + \sigma \pm 1)}{(\rho + \sigma)^2 - 1}.$$

Fig. 13— $v_1$  at cutoff ( $\theta=0$ ) as a function of slab thickness  
( $K = 1.52\pi$ ,  $\epsilon = 10$ ).

computed are indicated by the small circles. The curves are numbered according to the order of the modes of the completely filled waveguide starting with  $n=1$  for the first mode which cuts off at a positive (non-zero) value of  $v_1$ . The additional  $n=0$  (or  $v_1=0$ ) solution at  $\Delta=1$  is identified as being associated with the surface-wave mode. Points on the curves labeled  $n=2, 3, 4$  which lie in the shaded band are of no significance since values of  $v_1$  in the interval  $1-\rho < v_1 < 1$  do not occur. The bottom of this band ( $v_1=1-\rho$ ) corresponds to  $\sigma=0$ , the top ( $v_1=1$ ) to  $\sigma \rightarrow \infty$ . Since the cutoff characteristics depend on  $v_1$  only, a scale of numerical values for  $\sigma$  need not be given unless we choose to specify  $\rho$ . Therefore, in Fig. 13 we content ourselves with merely indicating the directions in which  $\sigma$  increases from zero to  $\sigma_5$  and decreases from infinity to  $\sigma_5$ .

There is a strong temptation to interpret the curves

in Fig. 4 as follows. The mode corresponding to any one curve is either propagating or cut off according to whether the point representing the values of  $v_1$  and  $\Delta$  lies "above" or "below" the curve.<sup>21</sup> While this interpretation does provide a rough idea of the conditions required for a particular mode to propagate, it is not strictly valid. The interpretation would be completely valid if the  $\theta$  vs  $\sigma$  characteristics for fixed  $\Delta$  (or, equivalently, the  $\theta$  vs  $\Delta$  characteristics for fixed  $\sigma$ ) were symmetrical about the  $\theta=0$  axis and were such that the poles of the derivative of  $\theta$  with respect to  $\sigma$  always coincided with  $\theta=0$ . The need for these reservations becomes apparent from an examination of the results indicated in, e.g., Fig. 17. Also, we remark that the curves in Fig. 13 give no indication of the erratic behavior of the solutions to (31) in the limit as  $\Delta \rightarrow 0$ . Therefore, they should not be used as a basis for a discussion of the cutoff characteristics in the immediate vicinity of  $\Delta=0$ .

The segment of the  $n=1$  curve shown with an expanded  $v_1$  scale at the top of Fig. 13 reveals that  $\Delta(v_1)$  for cutoff is multivalued for small positive  $\epsilon v_1$ . Presumably, this may also be the case for other values of  $n$  in the range of sufficiently small  $\epsilon v_1$ . The significance of this multivalued character becomes evident from a study of Figs. 14 and 15.<sup>22</sup> The curves in Fig. 14 are for  $v_1 < 0$  so that the only propagating modes are the surface wave mode ( $n=0$ ) and the perturbed empty waveguide mode ( $n=1$ ). The curves for both modes exhibit only the single cutoff predicted in Fig. 13. The manner in which the surface-wave mode disappears for  $\Delta \rightarrow 0$  and  $\Delta \rightarrow 1$  is consistent with the information given in (30). When  $v_1$  takes on small positive values corresponding to values of  $\sigma$  in the interval  $0 < \sigma < 1 - \rho$  the surface wave mode is still admitted for  $\Delta \neq 0, 1$ . The empty waveguide still propagates only the  $TE_{10}$  mode and, for sufficiently small  $v_1$ , the completely filled waveguide does not support any propagating modes. Now, it is evident from (30) that infinite solutions for  $\theta$  are no longer admitted with either  $\Delta \rightarrow 0$  or  $\Delta \rightarrow 1$ . Therefore, the only way in which the surface-wave mode can disappear at  $\Delta=0$  and  $\Delta=1$  is to have the  $\theta$  vs  $\Delta$  curve for this mode close on itself. This is precisely what happens in the curves labeled *a* and *b* in Fig. 15. In closing on itself, the  $\theta$  vs  $\Delta$  curve passes through  $\theta=0$  twice. Thus, the three values of  $\Delta$  at which Fig. 13 predicts that  $\theta$  will equal zero are all accounted for. As  $v_1$  is increased, the two separate  $\theta$  vs  $\Delta$  curves join to form a single continuous curve. This situation is illustrated by curve *c* of Fig. 15. When  $v_1$  is increased further to a value such that the completely filled waveguide will support one pair of propagating modes, the single curve *c* splits at  $\Delta=1$  to become the two continuous curves labeled *d*.

<sup>21</sup> In this connection, the adjective "above" is to be interpreted as implying "above and/or to the left of" for curves which vanish via  $v_1 \rightarrow -\infty$  and "above and/or to the right of" for the curves on which  $v_1$  tends to  $+\infty$ .

<sup>22</sup> Data for these curves was obtained by a graphical procedure described by Bresler (ref. 7).

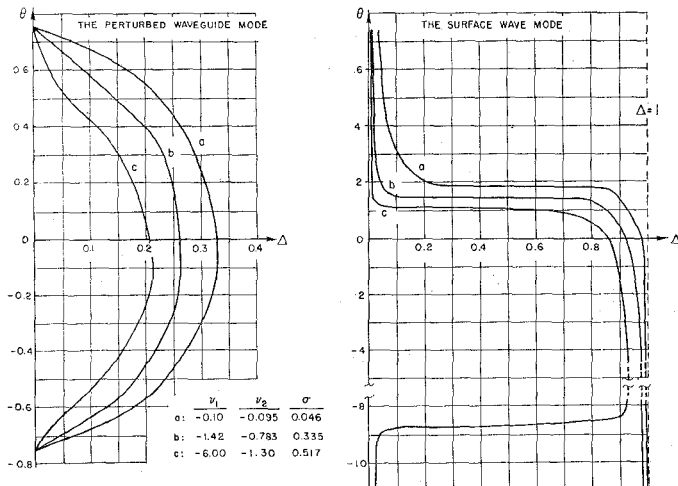


Fig. 14—Propagation constants as functions of the slab thickness  
 $(K = 1.52\pi, \epsilon = 10, \rho = 1)$ .

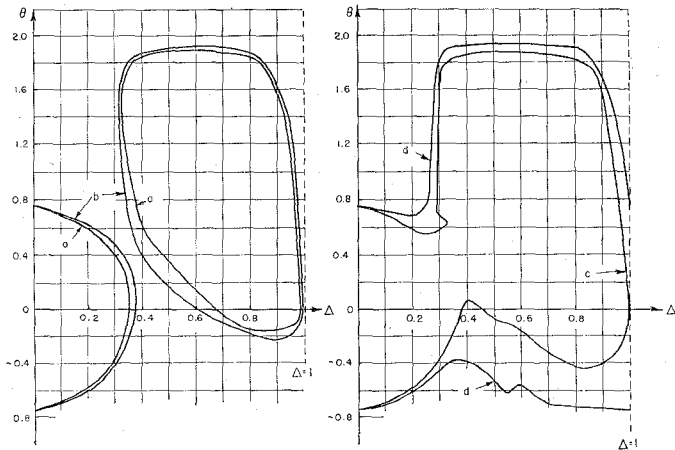


Fig. 15—Propagation constants as functions of the slab thickness  
 $(K = 1.52\pi, \epsilon = 10, \rho = 0.8)$ .

(a)  $\sigma = 0.190$ ,  $\nu_1 = 0.0245$ ,  $\nu_2 = 0.0249$ .  
 (b)  $\sigma = 0.1877$ ,  $\nu_1 = 0.0300$ ,  $\nu_2 = 0.0305$ .  
 (c)  $\sigma = 0.1822$ ,  $\nu_1 = 0.0433$ ,  $\nu_2 = 0.0444$ .  
 (d)  $\sigma = 0.1567$ ,  $\nu_1 = 0.100$ ,  $\nu_2 = 0.106$ .

When  $\nu_1$  is increased still further beyond the values employed in Fig. 15, additional propagating modes appear at  $\Delta = 1$  and will propagate for all values of  $\Delta$  down to approximately the cutoff value given in Fig. 13. As soon as  $\nu_1$  becomes reasonably large, the surface wave mode is no longer propagated by the ferrite-air interface, and therefore we are no longer required to account for either its presence or the manner of its disappearance at  $\Delta = 0, 1$ . Sketches of a typical set of  $\theta$  vs  $\Delta$  curves for a reasonably large value of  $\epsilon\nu_1$  are shown in Fig. 16.

The sketches shown in Fig. 17 illustrate the behavior of  $\theta$  as a function of  $\sigma$  for fixed  $\Delta$ . Certain essential features of these sketches (data concerning the surface-wave mode, the behavior at cutoff and the infinities in  $\theta$ ) follow directly from the results given above. Two other essential features (the slopes of the curves at  $\theta=0$  and the absence of maximum and minimum points)

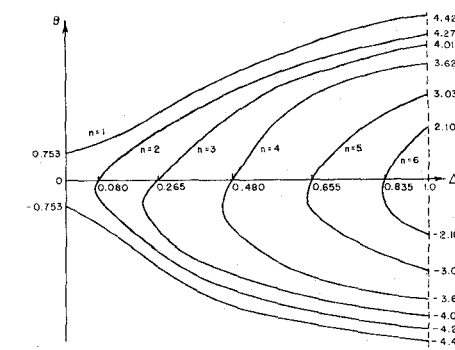
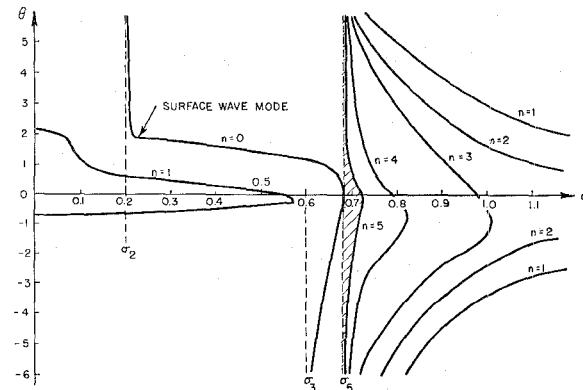
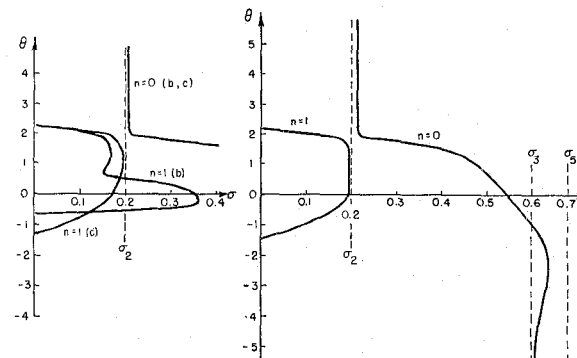


Fig. 16—Sketches of  $\theta$  vs  $\Delta$  for  $K = 1.52\pi$ ,  $\epsilon = 10$ ,  $v_1 = 2$ .



(a)



2), (c)

(d)

Fig. 17—Sketches of  $\theta$  vs  $\sigma$  for  $K=1.52 \pi$ ,  $\epsilon=10$ ,  $\rho=0.8$ .

(a)  $\Delta \approx 0.2$ , (b)  $\Delta \approx 0.3$ , (c)  $\Delta \approx 0.5$ , (d)  $\Delta \approx 0.9$ .

will be justified by the analysis presented in the next section.

The sketches in Fig. 17 are proportioned to correspond roughly to  $K=1.52\pi$ ,  $\epsilon=10$  and  $\rho=0.8$ . In Fig. 17(a), the region between the  $\sigma_5$  ordinate and the  $n=5$  curve is shaded to indicate that this region contains an infinity of propagating modes for each of which  $\theta\rightarrow\pm\infty$  as  $\sigma\rightarrow\sigma_5$  from above. The region corresponding to  $\sigma>\sigma_5$  is not reproduced in Fig. 17(b), (c), (d) since the basic characteristics of the  $\theta$  vs  $\sigma$  curves in this interval do not change with  $\Delta$ . In the interval  $0<\sigma<\sigma_5$  the  $n=0$  and  $n=1$  curves are shown for four different values of  $\Delta$ . The remainder of this paragraph is devoted to a simplified explanation for the behavior exhibited by

these sketches. For the values of  $\rho$  and  $\epsilon$  involved, an isolated ferrite-air interface would support a surface wave with  $\theta > 1$  throughout the interval  $0 < \sigma < \sigma_4$  where  $\sigma_4 > \sigma_2$ . With the finite thickness slab, the effect of placing the slab against a short circuiting wall is to convert the  $\sigma_2$  ordinate into a barrier which the  $\theta$  vs  $\sigma$  curve for the surface wave may not cross and at which  $\theta \rightarrow +\infty$  as  $\sigma \rightarrow \sigma_2$  from above. However, a study of Fig. 17 reveals that even with the smallest value of  $\Delta$  employed (*i.e.*, when the effect of the short circuit should be most pronounced) the surface wave reasserts itself as  $\sigma$  approaches zero and distorts the  $n=1$  curve so that part of this curve constitutes a continuation of the gently sloping portion of the  $n=0$  curve. As  $\Delta$  is increased so that the effect of the short circuit is diminished, the gap in the surface-wave characteristic between the  $n=0$  and  $n=1$  curves is likewise diminished. The gap does not disappear completely because the infinity at  $\sigma_2$  is required for any finite slab thickness.

#### THE POWER FLOW ASSOCIATED WITH THE PROPAGATING MODES

In an earlier paper<sup>6</sup> the author employed a matrix formulation for the Maxwell equations to deduce a relationship between the power flow associated with a propagating mode in an arbitrary dissipationless uniform waveguide and the frequency derivative of the propagation constant of this mode. For our purposes here, we require an analogous relationship involving the derivative of  $\theta$  with respect to  $\sigma$  when  $\rho$  and  $\omega$  (or  $k$ ) are held constant. By a procedure which parallels that employed in connection with (18) through (24) of the paper just cited,<sup>6</sup> it can be shown that the required relationship is

$$2P_\alpha\theta_\alpha' = \iint_S \mathbf{H}_\alpha^* \cdot \mathbf{u}' \cdot \mathbf{H}_\alpha dS \quad (33)$$

where  $\theta_\alpha$  is the (normalized) propagation constant of a particular propagating mode,  $P_\alpha$  is the (real) power flow associated with this mode,  $\mathbf{H}_\alpha$  is the total magnetic field of this mode,  $\mathbf{u}$  is the tensor permeability of the ferrite slab, the prime superscript indicates the derivative with respect to  $\sigma$  and the required integration is to be carried out over the cross section,  $S$ , of the waveguide.  $P_\alpha$  is defined so that it is positive for power flow along  $+z$ . The result in (33) is obtained when the modes are normalized in the manner indicated in the reference cited earlier.<sup>6</sup> Also, to obtain (33), we must exploit the fact that the boundary conditions at the waveguide walls, the (scalar) permittivity of the ferrite and both the (scalar) permeability and permittivity associated with the empty waveguide regions are all independent of  $\sigma$ .

For the  $TE_{n0}$  modes,  $\mathbf{H}_\alpha$  has nonzero components only in the plane transverse to  $y$  (*i.e.*, to  $H_0$ ). Therefore, for these modes, we introduce the subscript  $T$  to dis-

tinguish quantities confined to this transverse plane and rewrite (33) as

$$2P_\alpha\theta_\alpha' = \iint_S \mathbf{H}_{T\alpha}^* \cdot \mathbf{u}' \cdot \mathbf{H}_{T\alpha} dS. \quad (34)$$

For a dissipationless ferrite,  $\mathbf{u}'$  is a hermitian matrix, and therefore its derivative with respect to  $\sigma$  is also hermitian. Moreover, it is readily verified that (for fixed  $\rho$  and  $k$ ) this derivative is negative definite when  $\rho$  is positive. It then follows from (34) that for the  $TE_{n0}$  modes here under consideration

$$P_\alpha\theta_\alpha' < 0 \quad \text{for} \quad \rho > 0 \quad (35)$$

so that, for positive  $\rho$ ,  $P_\alpha \geq 0$  according as  $\theta_\alpha' \leq 0$ . Furthermore, we see that  $P_\alpha$  may equal zero only at the poles of  $\theta_\alpha'$ . This means that the power flow associated with a propagating mode can change direction only where  $\theta_\alpha'$  is infinite. A further important interpretation of (35) is the recognition that  $\theta_\alpha'$  can not equal zero unless  $P_\alpha$  becomes infinite. There is no difficulty in excluding the latter possibility in the case of closed waveguides, and we therefore conclude that  $\theta_\alpha' = 0$  cannot occur; *i.e.*, that the  $\theta$  vs  $\sigma$  curves cannot exhibit maximum or minimum points.

In the sketches in Fig. 17 we have indicated that the poles of  $\theta_\alpha'$  do not ordinarily occur where  $\theta_\alpha = 0$ . This statement is verified by noting that  $P_\alpha$  is zero only at the poles of  $\theta_\alpha'$  whereas it can be shown that<sup>7</sup> at  $\theta_\alpha = 0$

$$P_\alpha = -\frac{\nu_1^2}{K\nu_2} \left( \frac{\sin K\Delta \sqrt{\epsilon\nu_1}}{\sqrt{\epsilon\nu_1}} \right)^2. \quad (36)$$

Thus, for  $\theta_\alpha = 0$ , we find that  $P_\alpha \geq 0$  according as  $\nu_2 \leq 0$ . It then follows from (35) that, at  $\theta_\alpha = 0$ ,  $\theta_\alpha' \geq 0$  according as  $\nu_2 \geq 0$ . The availability of this last result eliminated a good deal of the guesswork which would otherwise have been involved in connection with the sketches in Fig. 17.

#### CONCLUSION—RESOLUTION OF THE THERMODYNAMIC PARADOX

It is evident from Fig. 17 that the possibility of the existence of only a single  $TE_{n0}$  propagating mode for the waveguide in Fig. 1 arises only from the fact that there is a nonvanishing interval between the values of  $\sigma$  at which  $\theta \rightarrow +\infty$  and  $\theta \rightarrow -\infty$  for the surface-wave mode. It is further evident that if this interval did not exist there would always be an even number of propagating modes. The results obtained in the preceding section, in particular, that in (35), make evident that this even number of propagating modes would always divide so that half transported energy in one direction along  $z$ , half in the other. This observation clears the way for the resolution of the thermodynamic paradox. It is reasonable to expect that the discontinuous behavior illustrated in Fig. 11 will also be evident for the surface-wave modes of the waveguides in Figs. 1 and 18. To verify this conjecture we note that the secular equation for the  $TE_{n0}$  modes of the latter waveguide is<sup>18</sup>

$$\begin{aligned}
 q_a \cot K(1 - \Delta - D)q_a + \frac{q_m}{\nu_1} \cot K\Delta q_m - \frac{\theta}{\nu_2} \\
 + \frac{\tan KDq_a}{q_a} \left\{ \left[ \frac{a_m}{\nu_1} \cot K\Delta q_m + \frac{\theta}{\nu_2} \right] q_a \cot K(1 - \Delta - D)q_a - \frac{q_m^2}{\nu_1^2} - \frac{\theta^2}{\nu_2^2} \right\} = 0 \quad (37)
 \end{aligned}$$

where  $D = d/a$ . The reader may verify that for any  $d \neq 0$ , however small, this equation admits both  $\theta \rightarrow \pm \infty$  as solutions for  $\sigma \rightarrow \sigma_3$  from above, and does not admit  $\theta \rightarrow +\infty$  as a solution in the neighborhood of  $\sigma_2$ . He may then further verify that, except for the discontinuity already referred to, all other solutions of (37) pass continuously into solutions of (24) in the limit as  $d \rightarrow 0$ . It will then be evident that in the limit as  $d \rightarrow 0$ , the sketches in Fig. 17 serve to describe all the modes of the waveguide in Fig. 18 except the  $n=0$  mode. A study of Fig. 11 makes evident that the  $\theta$  vs  $\sigma$  curve for the  $n=0$  mode of the waveguide in Fig. 18 will be that illustrated in Fig. 19. Finally, when we combine the results given in Figs. 17 and 19, we see that for any  $d \neq 0$  and, in particular, in the limit as  $d \rightarrow 0$ , the waveguide in Fig. 18 will always support an even number of propagating  $TE_{n0}$  modes. To establish that this conclusion is valid for values of  $K$  outside the range  $\pi < K < 2\pi$ , we need only recall that the locations of the infinities in  $\theta$  are independent of  $K$ .

The conclusion to which we are led is now evident. We have seen that if we accept the solutions of the secular equation (24) as constituting the correct description of the propagating  $TE_{n0}$  modes of the waveguide in Fig. 1, then we are led inescapably to a thermodynamic paradox. On the other hand, for any  $d \neq 0$  and, in particular, in the limit as  $d \rightarrow 0$ , the solutions of the secular equation (37) do not, *a priori*, give rise to any thermodynamic difficulties associated with the  $TE_{n0}$  spectrum of the waveguide in Fig. 18. These considera-

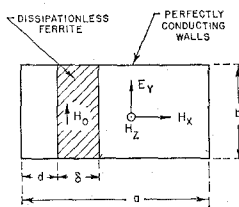


Fig. 18—Ferrite slab loaded rectangular waveguide (slab away from waveguide wall).

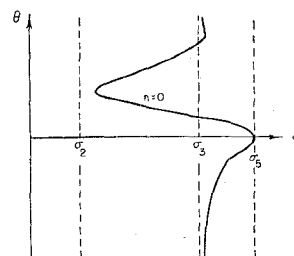


Fig. 19— $\theta$  vs  $\sigma$  for the surface wave mode of the waveguide in Fig. 18.

tions lead us to assert that the  $TE_{n0}$  mode propagation constants for the waveguide in Fig. 1 must be obtained from the solutions of the secular equation (37) in the limit  $d \rightarrow 0$  and not from the secular equation (24), *i.e.*, not from the secular equation which obtains at the limit  $d=0$ . We assert further that when this is done there will no longer exist any basis for construction of a thermodynamic paradox associated with the waveguide in Fig. 1.

The conclusion just stated may be criticized on the grounds that while it tells us how to avoid thermodynamic difficulties, it does not tell us why such difficulties are encountered. Anticipating such criticism, we offer the following remarks in our defense. The problem we have been considering is an idealization of a physical reality. Let us recall some of the idealizations which were implicit in our formulation of the problem. Thus, we have been considering absolutely dissipationless waveguides bounded by perfectly conducting walls and loaded with uniformly magnetized homogeneous ferrite slabs contained within sharply defined planar boundaries. All these idealizations are widely employed in the formulation of electromagnetic problems and we accept them on the basis of the implicit assumption that the solutions to these idealized problems represent the behavior of a physical system in an appropriate limiting sense. To speak of the ferrite slab in Fig. 18 as being against the waveguide wall is to describe a physical situation for which we can not ordinarily distinguish between the mathematical descriptions  $d=0$  and the limit as  $d \rightarrow 0$ . Given two different but equally acceptable mathematical idealizations for a physical situation, we are often called upon to distinguish between these idealizations by the physical content of the solutions to the problem which they yield. Thus, in our problem, we find that the two idealizations  $d=0$  and  $d \rightarrow 0$  lead to distinctly different solutions. Without asking why this difference arises, we are justified in choosing between them on the basis that the idealization which leads to a thermodynamic paradox must be discarded.

#### ACKNOWLEDGMENT

The author wishes to express his gratitude to his thesis adviser, Prof. N. Marcuvitz, for his guidance and assistance. Also, the author is indebted to his colleagues at the Microwave Research Institute, in particular to Prof. J. Shmoys, for their numerous helpful discussions and criticisms. Finally, thanks are due to Miss J. Spector for her perseverance in carrying out the tedious computations.